Contents lists available at ScienceDirect

Journal of Alloys and Compounds

journal homepage: www.elsevier.com

Engineering of magnetically separable $ZnFe_2O_4$@ TiO_2 nanofibers for dye-sensitized solar cells and removal of pollutant from water

Saeed Al-Meer[a, *, 1], Zafar Khan Ghouri[a, **, 1], Khaled Elsaid[b], Ahmed Easa[a], Muneera Th. Al-Qahtani[a], M. Shaheer Akhtar[c, ***]

[a] Central Laboratories Unit, Qatar University, P. O. Box: 2713, Doha, Qatar
[b] Chemical Engineering Program, Texas A&M University at Qatar, P. O. Box: 23874, Doha, Qatar
[c] New & Renewable Energy Material Development Center (NewREC), Chonbuk National University, Jeonju, 54896, Republic of Korea

ARTICLE INFO

Article history:
Received 19 April 2017
Received in revised form 19 June 2017
Accepted 20 June 2017
Available online xxx

Keywords:
Zinc ferrite
Electrospinning
Hydrothermal method
Photoanode
Solar cells
Photocatalyst

ABSTRACT

In this study, magnetic Zinc Ferrite ($ZnFe_2O_4$)@TiO_2 nanofibers were prepared by low cost and nontoxic route; hydrothermal technique followed by electrospinning process. The prepared magnetic $ZnFe_2O_4$@TiO_2 nanofibers were morphologically and structurally analyzed by X-ray diffractometer (XRD), Fourier transform infrared spectroscopy (FTIR), field emission scanning electron microscope (FESEM), transmission electron microscope (TEM), and thermal gravimetric analysis (TGA). The prepared magnetic $ZnFe_2O_4$@TiO_2 nanofibers were utilized as photoanode for the fabrication of dye-sensitized solar cells (DSSCs) and presented applicable performance with 4.2% overall conversion efficiency with high short circuit current density (J_{SC}) of 10.16 mA/cm^2. The maximum ~42% incident photo-to-current conversion efficiency (IPCE) value was also recorded at 520 nm. In addition, $ZnFe_2O_4$@TiO_2 nanofibers were not only possessed the good conversion efficiency, but also shown excellent photocatalytic efficiency with magnetic properties towards the dye remediation. Prepared $ZnFe_2O_4$@TiO_2 nanofibers can be considered as a promising material for energy conversion and environmental applications.

1. Introduction

Due to accumulative worldwide energy demand and exhaustion of fossil oil resources and environmental concerns have undoubtedly become the greatest problems attracting worldwide attention over the past decades [1,2]. One of the sustainable and green, everlasting and economical energy sources are the sun [3]. In every 60 min, the sunlight knockouts to the earth giving energy more than sufficient to fulfill worldwide energy needs for an entire year [3,4]. The supply of solar energy from the sun to the earth is about 3×10^{24} J/Year, which would amount to 10^4 times of mankind energy consumption [5]. Solar energy is one of the most promising technologies used to yoke sun's energy and make it useable [6]. Solar energy can be transformed to electrical energy by several ways; solar cell is one of these, especially for (i) mass production, (ii) high efficiency and (iii) various applications [7]. Besides a lot of merits, there are some drawbacks that come with it, such as high cost and requirement of wide area to fix the solar panel [7].

Dye sensitized solar cells (DSSCs) have appeared as a prospective alternative to conventional silicon-based solar cell with numerous advantages like high conversion efficiency at low manufacturing cost [8–10]. DSSCs classically construct with metal oxides semiconductors as photo anode, organic sensitized dyes, electrolyte (usually based on the I_3^-/I^- redox couple), and counter electrode (e.g. Pt) in the sandwich form [8]. The two main hindrances such as slow electron transport rate and the energy losses caused by the recombination in DSSCs need to be overcome for high performance [11,12]. To address these technological challenges, many attempts were made by replacing or improving morphology and surface properties of the conventional TiO_2 photoanode materials [13–15]. The fibrous nature of TiO_2 materials generally provides the high surface to volume ratio which might considerably helpful for high dye absorption over the TiO_2 electrode. Recently, a simple electrospinning offers cost effective technique to develop well controlled nanofibers with wide range of average diameter (50–500 nm) [16]. Recently, the addition and doping on TiO_2 nanofibers show the many advantages like the reduction in band gap, arrangement of new states in the energy forbidden region, high generation of charge carriers concentration in the conduction band, which collectively enhance the absorption of the solar spectrum [17–19].

On the other hand, there has been a great interest in developing photocatalysts for remediation of hazardous organic compounds in industrial wastewater [20,21]. Textile dyestuffs are one of the most common organic pollutants in industrial wastewater. One of these dyes methylene blue is not only toxic but also causes serious environ-

* Corresponding author.
** Corresponding author.
*** Corresponding author.
Email addresses: salmeer@qu.edu.qa (S. Al-Meer); zafarkhan.ghouri@qu.edu.qa, zafarkhanghouri@hotmail.com (Z.K. Ghouri); shaheerakhtar@jbnu.ac.kr (M. Shaheer Akhtar)

[1] Dr. Zafar Khan Ghouri and Dr. Saeed Al-Meer have contributed equally to this work.

http://dx.doi.org/10.1016/j.jallcom.2017.06.211
0925-8388/

mental problems and damage the aquatic life [22]. Numerous physical and chemical techniques have been applied for the removal of dyes from industrial wastewater. Among them, the heterogeneous photocatalytic process is an authentic technique, which can be successfully used to degrade the organic pollutants. In particular, one-dimensional TiO_2 nanostructures such as TiO_2 nanowires, TiO_2 nanorods and TiO_2 nanofibers show higher catalytic activities than that TiO_2 nanoparticles in various photocatalysis because the photo-generated electrons frequently encountered massive amounts of grain boundaries among the nanoparticles (NPs). In this condition, transportation of electron is limited with high probability of recombination. However, grain boundaries effect can also be restricted by using TiO_2 nanofibers based catalysts [8,23]. Moreover, among the spinel ferrite compounds Zinc Ferrite ($ZnFe_2O_4$), a semiconductor shown to be a promising inorganic sensitizer for TiO_2 photocatalyst because it could not only efficiently extent the photoresponse of TiO_2 under wide region of solar light but facilitates the separation of photo-induced charges and lowering the charge transfer resistance [24–26]. Thus, the incorporation of trace impurities of $ZnFe_2O_4$ into TiO_2 nanofibers had a great effect on improving the overall photocatalytic efficiency [6,12,27–30].

In this study, two-steps method has been employed to synthesize the bi-functional magnetic Zinc Ferrite ($ZnFe_2O_4$) @ TiO_2 nanofibers. In first step, pristine TiO_2 nanofibers have been prepared using simple, low cost and effective technique; electrospinning. Secondly, $ZnFe_2O_4$ was doped on TiO_2 nanofibers by widely used, simple, low cost and nontoxic route; hydrothermal technique using $Zn(NO_3)_2$ and $FeCl_3$ precursor. The physicochemical characterizations have been investigated in term of morphology and crystallinity. Finally, magnetic $ZnFe_2O_4$@ TiO_2 nanofibers were applied as photoanode for DSSCs and achieved ∼4.2% energy conversion efficiency. Moreover, the magnetic $ZnFe_2O_4$@ TiO_2 nanofibers as catalyst showed a superior photodegradation activity for organic dye.

2. Experimental

2.1. Materials

Poly-vinyl pyrrolidone (PVP) with molecular weight 130,000 g/mol, titanium (IV) Isopropoxide (TTIP, 97%), iron(III)chloride ($FeCl_3$) 97% reagent grade), zinc nitrate hexahydrate ($Zn(NO_3)_2{\cdot}H_2O$) 98% reagent grade), Polyethylene glycol (PEG) were purchased from Sigma–Aldrich, USA and acetic acid (CH_3COOH) reagent grade) were purchased from Showa Chemicals Co. Ltd., Japan.

2.2. Preparation of TiO_2 nanofibers

Based on our previous studies [31], TiO_2 nanofibers were prepared with the electrospinning technique. Briefly, a sol-gel was achieved by mixing of 1.5 g of titanium (IV) Isopropoxide and 0.45 g of Poly-vinyl pyrrolidone with few drops of acetic acid. After stirring at room temperature 4 g of polyethylene glycol (PEG) was added and stirred at the same condition. The resulting transparent solution was electrospun and initially vacuum dried at 60 °C for 12 h and finally calcined in air atmosphere at 600 °C for 3 h.

2.3. Preparation of magnetic $ZnFe_2O_4$@ TiO_2 nanofibers

In order to synthesize magnetic $ZnFe_2O_4$@ TiO_2 nanofibers, 100 mg of TiO_2 nanofibers, 80 mg $FeCl_3$ and 80 mg of $Zn(NO_3)_2{\cdot}H_2O$ are mixed together in 25 ml deionized water under vigorous stirring, and then 5–6 drops of PEG were added and kept stirring for 45 min. The mixture was transferred into 120 ml Teflon container jacketed with stainless-steel autoclave and baked at temperature of 180 °C for 8 h. Finally, the mixture was filtered and washed with distilled water many times then dried at 80 °C for 24 h to obtain magnetic $ZnFe_2O_4$@ TiO_2 nanofibers.

2.4. Characterization and photocatalytic measurements

Information about the phase structure and crystallinity was determined by powder X-ray diffraction spectrum (XRD, Rigaku Japan) with Cu-Kα (λ = 1.54056 Å) radiation operating at 45 kV and 100 mA over a range of 2θ angle from 10° to 80°, scanning at a rate of 4°/min. The morphology of the as-prepared sample was examined with field-emission scanning electron microscopy (FESEM, Hitachi S-7400, Japan). TEM images were observed by JEOL JEM-2200FS transmission electron microscope (TEM) operating at 200 kV (JEOL, Japan). The spinel structure was examined through PerkinElmer (USA), Spectrum 400 FT-IR/FT-NIR spectrometer while thermal properties of the as-prepared sample was examined through PerkinElmer (USA), Pyris6 TGA, from room temperature to 800 °C under nitrogen environment at the heating rate of 10 °C/min. The procedure used for fabrication and measurements of DSSCs in this study have followed according to our previously literatures [32]. While photocatalytic efficiency of synthesized magnetic $ZnFe_2O_4$@ TiO_2 nanofibers was assessed under natural environment on sunny day at average ambient temperature and mean daily global solar radiation, of about 25–30 °C and 489.3 mWh/cm^2, respectively in March between 01:00 p.m. and 3:0 p.m. by degradation of methylene blue dye. First, 20 mg of synthesized magnetic $ZnFe_2O_4$@ TiO_2 nanofibers was socked in reaction flask containing 50 ml of (10 ppm) methylene blue aqueous solution. The suspension was then exposed to the sunlight under vigorous stirring; 2 ml of aliquots were then taken regularly from the reaction flask. After removal of dispersed photocatalyst the change in the methylene blue concentration was checked by UV–Vis spectrometer (absorbance, 200–900 nm).

3. Results and discussion

The crystal structure of the synthesized magnetic $ZnFe_2O_4$@ TiO_2 nanofibers was identified by X-Ray diffraction (XRD) measurement and the results are shown in Fig. 1. As shown in the figure, some well-defined diffraction peaks at 2θ of 27.19°, 35.69°, 40.80° and 68.27° correspond to the crystal planes of (110), (101), (111) and (301), respectively are observed. These peaks correspond to a tetragonal rutile phase of TiO_2 [space group: *P*42/*mnm* (136)] according to the joint committee on powder diffraction standards (JCPDS) file No. 01-076-0322] with lattice constants $a = b = 4.6344$ Å, $c = 2.9919$ Å; $\alpha = \beta = \gamma = 90$. It is quite common that the metal precursors fused together to form alloys structure. The XRD result confirms that $Zn(NO_3)_2$ dissolved in some $FeCl_3$ to form $ZnFe_2O_4$ (Franklinite). Various diffraction peak located at 2θ of 29.9°, 35.3°, 42.9°, 53.2°, 56.7°, 62.2° and 73.5° are well indexed to the (220), (311), (400), (420), (511), (440) and (533) lattice planes respectively, and indexed to Fd3m cubic spinel structure of $ZnFe_2O_4$ (JCPDS file No. 22–1012), which confirms that $ZnFe_2O_4$ have been well decorated on the TiO_2 nanofibers during the proposed synthesis route.

The morphologies of the synthesized magnetic Zinc Ferrite ($ZnFe_2O_4$) @ TiO_2 nanofibers after carbonization were characterized by FE-SEM and TEM analysis. As shown in Fig. 2 (a), pristine TiO_2 electrospun nanofibers exhibit smooth and bead-free morphology. Fig. 2 (b) shows the FE-SEM image of hydrothermally synthesized

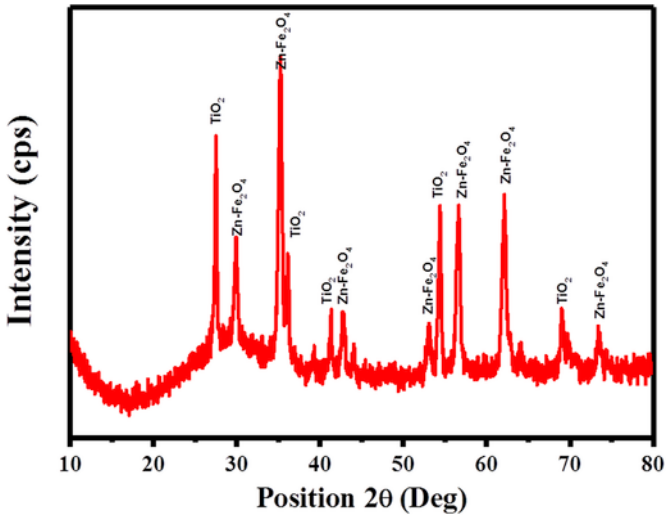

Fig. 1. XRD pattern for the obtained magnetic Zinc Ferrite ($ZnFe_2O_4$)@TiO_2 nanofibers.

magnetic Zinc Ferrite ($ZnFe_2O_4$) @ TiO_2 nanofibers. After the hydrothermal treatment at 180 °C for 8 h, the nano-dodecahedron crystals of $ZnFe_2O_4$ grow and densely dotted along the entire surface of TiO_2 nanofibers.

Chemical composition was analyzed by SEM-EDX, as shown in SEM image (Fig. 2(c & d)) with corresponding EDX, of magnetic Zinc Ferrite ($ZnFe_2O_4$) @ TiO_2 nanofibers is purely made of Zn, Fe, Ti and O. The atomic and weight percentage of Zn, Fe, Ti and O are summarized in the inset in Fig. 2(d). Additional confirmation and distribution of Zn, Fe, Ti and O is provided by TEM line EDX and elemental mapping of the specific area, as shown in the main images and their corresponding concentration profiles (Fig. 3(a and b)), Zn, Fe and O are evenly distributed over the entire surface of nanofibers.

Fig. 4(a & b) displays TEM and corresponding HR-TEM images of the synthesized magnetic $ZnFe_2O_4$@ TiO_2 nanofibers after carbonization. As shown in Fig. 4 (a), the nano-crystal of $ZnFe_2O_4$ is adhered on the surface of TiO_2 nanofiber while corresponding HR-TEM image (Fig. 4(b)) shows that the attached nano-crystals have good crystallinity. Moreover, the selected area electron diffraction pattern (SEAD, (Fig. 4(c)) indicates that the appearance of multilayer patterns is related to polycrystalline nature of grown $ZnFe_2O_4$@ TiO_2 nanofibers.

To investigate the spinel structure of magnetic $ZnFe_2O_4$@ TiO_2 nanofibers, FTIR spectrum was recorded through. As shown in Fig. 5, two characteristics absorption peaks at about 466 cm^{-1} and 1100 cm^{-1} are belongs to Ti-O stretching [33,34]. Furthermore, the absorption peaks at around 550 cm^{-1} can be assigned to tetrahedral Zn-O bonds while absorption peak at around 415 cm^{-1} can be associated to octahedral Fe-O bonds [35,36].

Thermal properties were measured from room temperature to 800 °C by TGA. Three main weight losses are observed (Fig. 6). As shown, the first loss takes place at ~ 70 °C to 150 °C with mass loss of ~20% is related to the desorption of physically adsorbed water and solvent loss (ethanol and acetic acid) [37]. Second weight loss at ~ 250 °C were due to simultaneous decomposition of TIP and PVP polymer while weight loss observed at ~600 °C is due to the dehydration of structural water and phase transformation [37–39]. In addition, obvious weight loss is also observed after 800 °C, which indicates that the thermal stability of the composite is very high, which is acceptable due to an effect of different oxides used whose phases are different therefore; the thermal stability also will be different. Thus, overall thermal stability of composite is higher than 800 °C.

The synthesized magnetic $ZnFe_2O_4$@ TiO_2 nanofibers have been utilized as photoanode for the fabrication of DSSC and evaluated the

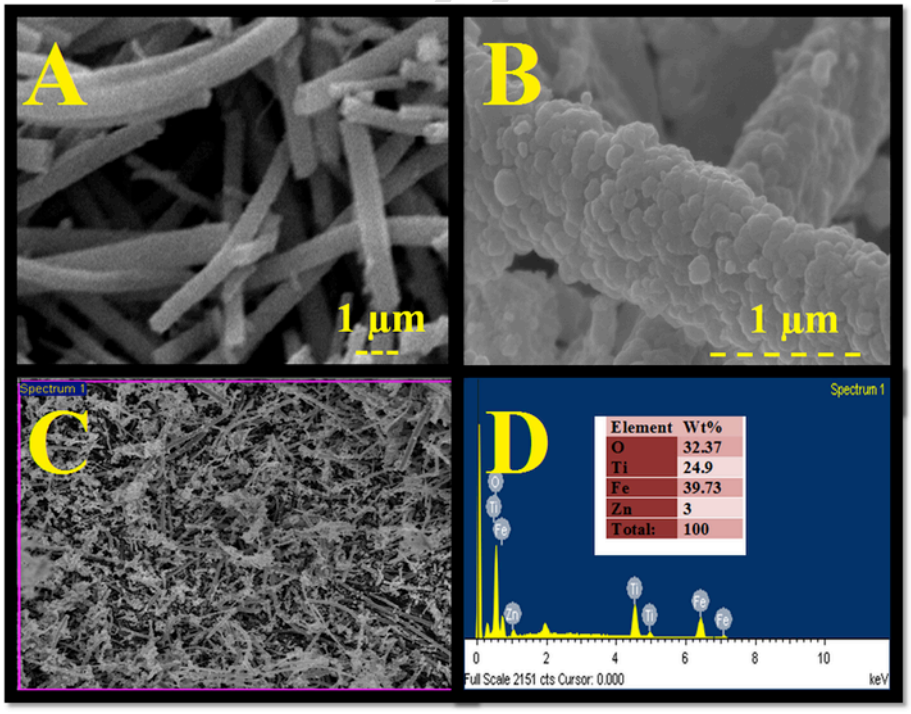

Fig. 2. (a) FESEM image of pristine TiO_2 nanofibers, (b & c) SEM image with corresponding EDS maps (d) for Zn, Fe, O and Ti for the obtained magnetic Zinc Ferrite ($ZnFe_2O_4$)@TiO_2 nanofibers.

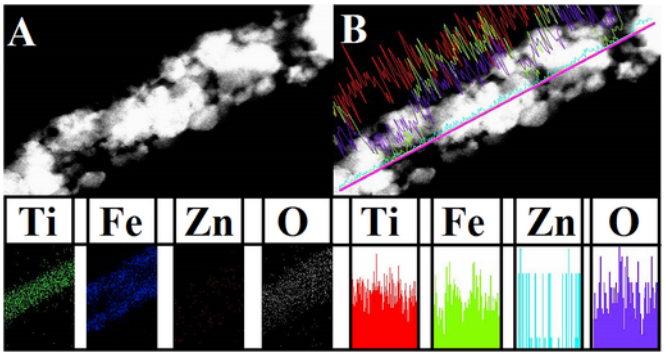

Fig. 3. (a) Elemental mapping and (b) Line EDX for the obtained magnetic Zinc Ferrite ($ZnFe_2O_4$)@TiO_2 nanofibers.

photovoltaic performance by measuring photocurrent–voltage (I–V) curve under light illumination with 100 mW/cm^2 (AM 1.5) light intensity. The photovoltaic responses of the fabricated DSSCs have been estimated in term of short-circuit photocurrent density (J_{SC}), open-circuit voltage (V_{OC}), fill factor (FF), and energy conversion efficiency (η). The conversion efficiency (η) was calculated through the following equation.

$$\eta = \frac{J_{SC} V_{OC} FF}{P_{in}} \quad (1)$$

where, P_{in} is the intensity of the incident light.

As shown in Fig. 7(a), the synthesized magnetic $ZnFe_2O_4$@TiO_2 nanofibers based photoanode reveals the higher conversion efficiency of 4.2% than pristine TiO_2 nanofibers based photoanode (η = 3.2%), which is considerably higher by about 24% with respect to the pristine TiO_2 nanofibers based DSSCs. The improved energy conversion efficiency accredited to the higher Voc = 0.767 V and Jsc = 10.16 mA/cm^2, that are considerably higher than those of pristine TiO_2 based photoanode. The improved conversion efficiency of magnetic $ZnFe_2O_4$@ TiO_2 nanofibers based DSSCs could not only be attributed to distinctive structure but also from the incorporation of $ZnFe_2O_4$ that have comparatively small band-gap energy (1.9 eV) [24]. Obviously, $ZnFe_2O_4$ can promotes the photoresponse of TiO_2 nanofibers to the visible light region and thus improve the utilization of solar light. Moreover, $ZnFe_2O_4$ can provides a path to help the charge transfer from the excited dye to the conduction band of the photoanode [40].

Incident photon to current conversion efficiency (IPCE) or external quantum efficiency (EQE) is a function of wavelength used to measure the conversion (incident light into electrical energy at a given wavelength) efficiency of device and it can be expressed through eq. (2)

$$IPEC(\lambda) = LHE(\lambda)\,\phi_{inj}\eta_{col} \quad (2)$$

where, LHE (λ) is the light harvesting efficiency for photons of wavelength λ, ϕ_{inj} is the quantum yield for electron injection from the excited sensitizer into the conduction band of the photoanode oxide, and λ_{col} is the electron collection efficiency. Fig. 7(b) shows IPCE data, as shown in the obtained spectrum, the photoanode covers wide range of solar spectrum for absorbing light to produce photocurrent. This credited of their advantageous band gap for optimum light harvesting. Moreover, the maximum IPCE value of 42% is achieved at 530 nm.

On the other hand, the typical photocatalytic activity of synthesized magnetic $ZnFe_2O_4$@ TiO_2 nanofibers under the solar light irradiation has been performed. Methylene blue (MB) dye was utilized as an exemplary pollutant and the degradation percentage (%) of MB was calculated by the following equation.

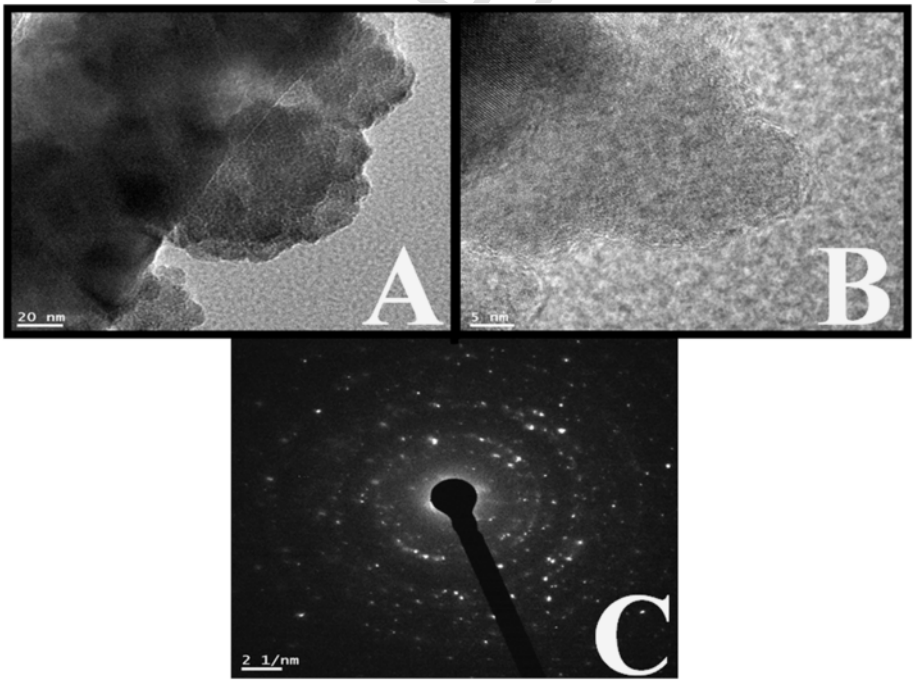

Fig. 4. (a) TEM, (b) HR-TEM image and (c) SEAD image for the obtained magnetic Zinc Ferrite ($ZnFe_2O_4$)@TiO_2 nanofibers.

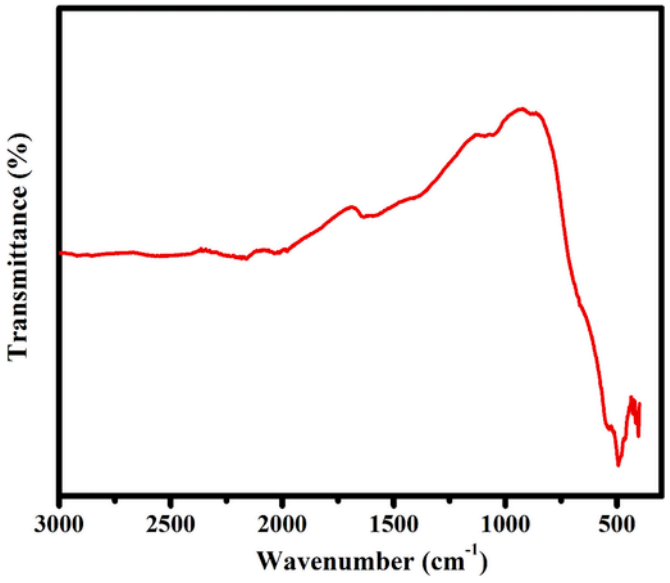

Fig. 5. FTIR pattern for the obtained magnetic Zinc Ferrite ($ZnFe_2O_4$)@TiO_2 nanofibers.

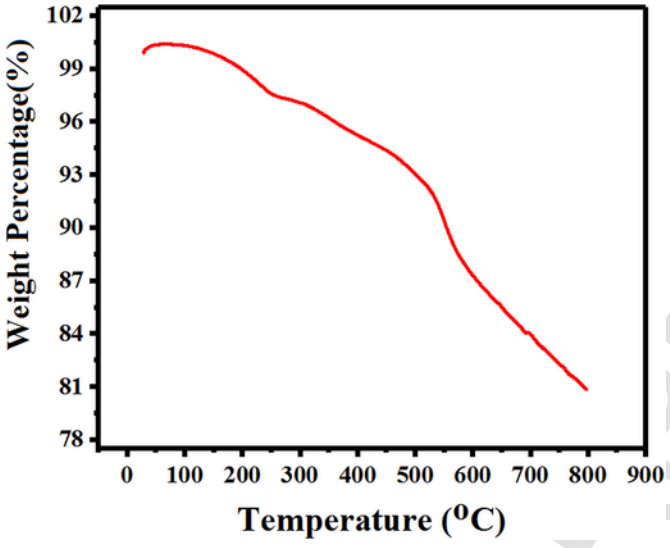

Fig. 6. TGA pattern for the obtained magnetic Zinc Ferrite ($ZnFe_2O_4$)@TiO_2 nanofibers.

$$Degradation\,(\%) = \frac{C_\circ - C}{C_\circ} 100 \qquad (3)$$

where, $C_\circ$ and C are the initial and final concentrations of MB respectively. As shown in Fig. 8 (a), more than 80% of the MB dye is removed just in 40 min and the complete removal of MB dye is recorded within 1 h (shown in digital image Fig. 8 (b)). It can be explained by the synergetic effect developed in between narrow band gap semiconductor ($ZnFe_2O_4$) and wide band gap TiO_2 nanofibers, which eased the transportation efficiency of photogenerated electron at the interface of the coupled semiconductor system ($ZnFe_2O_4$@TiO_2) [41,42], resulting in the rapid degradation of MB dye under visible light illumination. (Fig. 8 (b)). In addition, the synthesized nanostructures can be easily collected through external magnetic field (Fig. 8(b)).

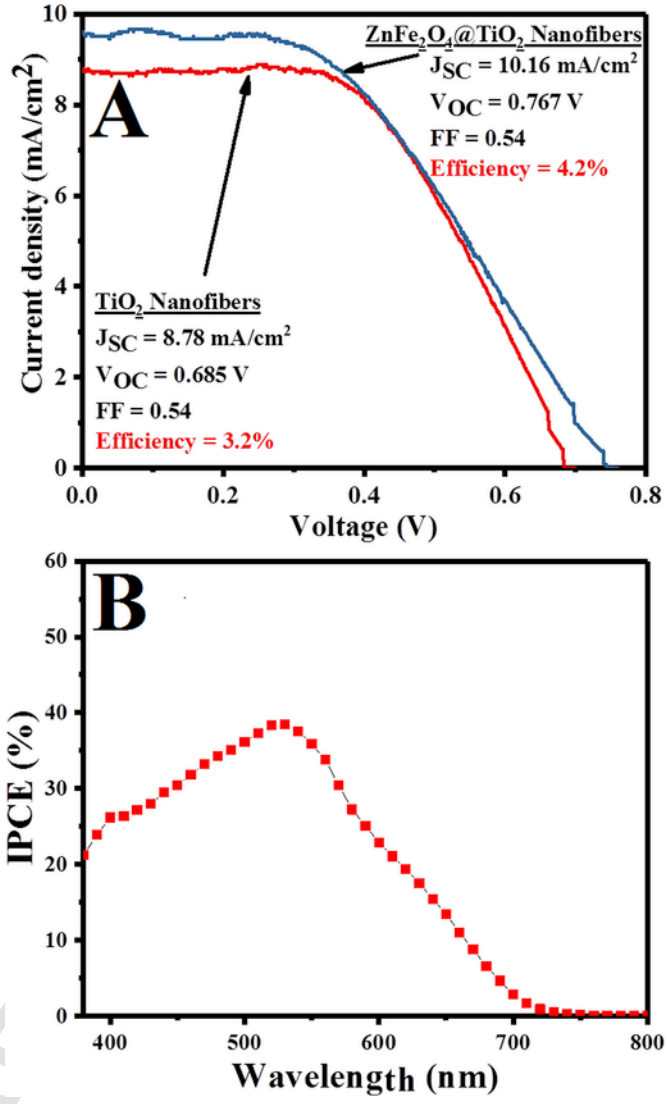

Fig. 7. (a) Performance of obtained magnetic Zinc Ferrite ($ZnFe_2O_4$)@TiO_2 and pristine TiO_2 nanofibers as photoanode in DSSCs, (b) External quantum efficiency of DSSCs based on magnetic Zinc Ferrite ($ZnFe_2O_4$)@TiO_2 nanofibers photoanode.

4. Conclusions

The introduced magnetic $ZnFe_2O_4$@ TiO_2 nanofibers show satisfactory performance as photoanode for DSSCs and also own the excellent photocatalytic properties. XRD, FE-SEM and TEM characterizations reveal that $ZnFe_2O_4$ is formed over the surface of TiO_2 nanofibers. The magnetic $ZnFe_2O_4$@ TiO_2 nanofibers based photoanode displays the higher conversion efficiency of 4.2% which is considerably improved by about 24% as compared to the pristine TiO_2 nanofibers based DSSCs. Moreover, magnetic $ZnFe_2O_4$@ TiO_2 nanofibers present rapid photocatalytic MB dye degradation in very short time. A notable magnetic property reveals its multifunctional activity and can serve as a promising material for energy and environmental applications.

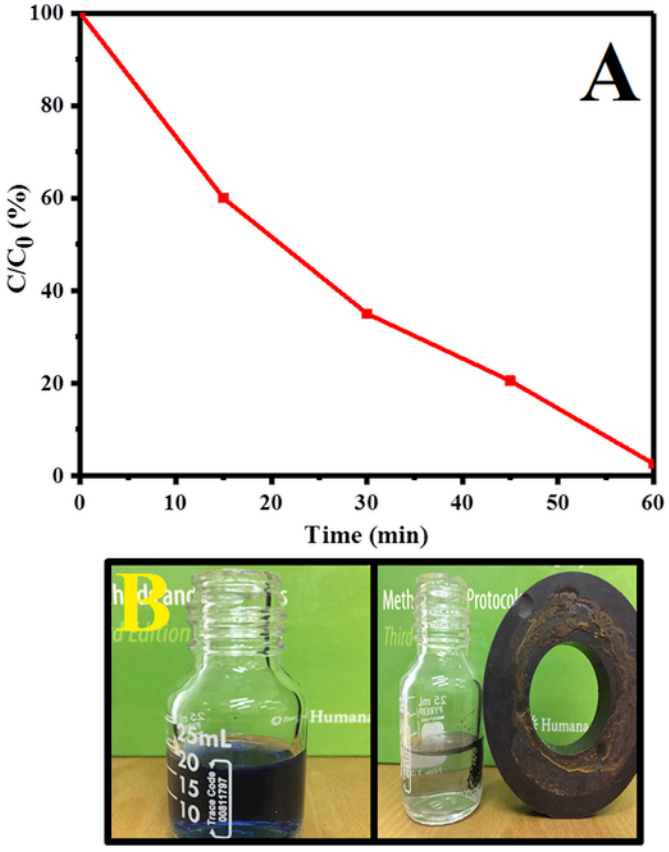

Fig. 8. (a) Photocatalytic degradation of MB aqueous solution under solar light irradiation (b) digital images magnetic Zinc Ferrite ($ZnFe_2O_4$)@TiO_2 nanofibers photocatalysts under an external magnetic field.

Acknowledgments

Dr. Zafar Khan Ghouri gratefully acknowledges the support of central laboratories Unit, Qatar University.

References

[1] Z.K. Ghouri, N.A. Barakat, H.Y. Kim, Influence of copper content on the electrocatalytic activity toward methanol oxidation of CoχCuy alloy nanoparticles-decorated CNFs, Sci. Rep. 5 (2015).
[2] Z.K. Ghouri, N.A. Barakat, A.-M. Alam, M.S. Alsoufi, T.M. Bawazeer, A.F. Mohamed, H.Y. Kim, Synthesis and characterization of Nitrogen-doped &Ca-CO3-decorated reduced graphene oxide nanocomposite for electrochemical supercapacitors, Electrochim. Acta 184 (2015) 193–202.
[3] D. Susanti, M. Nafi, H. Purwaningsih, R. Fajarin, G.E. Kusuma, The preparation of dye sensitized solar cell (DSSC) from TiO2 and tamarillo extract, Proced. Chem. 9 (2014) 3–10.
[4] W. David Wei, J.S. DuChene, B.C. Sweeny, J. Wang, W. Niu, Chapter 12-current development of photocatalysts for solar energy conversion A2-suib, steven L, In: New and Future Developments in Catalysis, Elsevier, Amsterdam, 2013, pp. 279–304.
[5] B. Li, L. Wang, B. Kang, P. Wang, Y. Qiu, Review of recent progress in solid-state dye-sensitized solar cells, Sol. Energy Mater. Sol. Cells 90 (2006) 549–573.
[6] K. Deepa, P. Lekha, S. Sindhu, Efficiency enhancement in DSSC using metal nanoparticles: a size dependent study, Sol. Energy 86 (2012) 326–330.
[7] H. Ferhati, F. Djeffal, F. Srairi, Enhancement of the absorbance figure of merit in amorphous-silicon p-i-n solar cell by using optimized intermediate metallic layers, Optik - Int. J. Light Electron Opt. 130 (2017) 473–480.
[8] P. Joshi, L. Zhang, D. Davoux, Z. Zhu, D. Galipeau, H. Fong, Q. Qiao, Composite of TiO 2 nanofibers and nanoparticles for dye-sensitized solar cells with significantly improved efficiency, Energy & Environ. Sci. 3 (2010) 1507–1510.
[9] B. O'regan, M. Grfitzeli, A low-cost, high-efficiency solar cell based on dye-sensitized, Nature 353 (1991) 737–740.
[10] T.W. Hamann, R.A. Jensen, A.B. Martinson, H. Van Ryswyk, J.T. Hupp, Advancing beyond current generation dye-sensitized solar cells, Energy & Environ. Sci. 1 (2008) 66–78.
[11] Q. Huang, G. Zhou, L. Fang, L. Hu, Z.-S. Wang, TiO2 nanorod arrays grown from a mixed acid medium for efficient dye-sensitized solar cells, Energy & Environ. Sci. 4 (2011) 2145–2151.
[12] M. Wang, Y. Wang, J. Li, ZnO nanowire arrays coating on TiO 2 nanoparticles as a composite photoanode for a high efficiency DSSC, Chem. Commun. 47 (2011) 11246–11248.
[13] M.Y. Song, D.K. Kim, K.J. Ihn, S.M. Jo, D.Y. Kim, Electrospun TiO2 electrodes for dye-sensitized solar cells, Nanotechnology 15 (2004) 1861.
[14] M. Adachi, Y. Murata, J. Takao, J. Jiu, M. Sakamoto, F. Wang, Highly efficient dye-sensitized solar cells with a titania thin-film electrode composed of a network structure of single-crystal-like TiO2 nanowires made by the "oriented attachment" mechanism, J. Am. Chem. Soc. 126 (2004) 14943–14949.
[15] S.C. Yang, D.J. Yang, J. Kim, J.M. Hong, H.G. Kim, I.D. Kim, H. Lee, Hollow TiO2 hemispheres obtained by colloidal templating for application in dye-sensitized solar cells, Adv. Mater. 20 (2008) 1059–1064.
[16] N.A. Barakat, M. Motlak, A.A. Elzatahry, K.A. Khalil, E.A. Abdelghani, Ni x Co 1− x alloy nanoparticle-doped carbon nanofibers as effective non-precious catalyst for ethanol oxidation, Int. J. Hydrogen Energy 39 (2014) 305–316.
[17] Y. Horie, T. Watanabe, M. Deguchi, D. Asakura, T. Nomiyama, Enhancement of carrier mobility by electrospun nanofibers of Nb-doped TiO 2 in dye sensitized solar cells, Electrochim. Acta 105 (2013) 394–402.
[18] N. Massihi, M. Mohammadi, A. Bakhshayesh, M. Abdi-Jalebi, Controlling electron injection and electron transport of dye-sensitized solar cells aided by incorporating CNTs into a Cr-doped TiO 2 photoanode, Electrochim. Acta 111 (2013) 921–929.
[19] M. Motlak, M.S. Akhtar, N.A. Barakat, A. Hamza, O.-B. Yang, H.Y. Kim, High-efficiency electrode based on nitrogen-doped TiO 2 nanofibers for dye-sensitized solar cells, Electrochim. Acta 115 (2014) 493–498.
[20] S. Ameen, M.S. Akhtar, H.S. Shin, ZnO hollow nano-baskets for mineralization of cationic dye, Mater. Lett. 183 (2016) 329–333.
[21] S. Ameen, M.S. Akhtar, H.-K. Seo, H.-S. Shin, Solution-processed CeO 2/TiO 2 nanocomposite as potent visible light photocatalyst for the degradation of bromophenol dye, Chem. Eng. J. 247 (2014) 193–198.
[22] S. Ameen, M.S. Akhtar, H.-K. Seo, H.S. Shin, Advanced ZnO–graphene oxide nanohybrid and its photocatalytic applications, Mater. Lett. 100 (2013) 261–265.
[23] B. Liu, E.S. Aydil, Growth of oriented single-crystalline rutile TiO2 nanorods on transparent conducting substrates for dye-sensitized solar cells, J. Am. Chem. Soc. 131 (2009) 3985–3990.
[24] G. Song, F. Xin, X. Yin, Photocatalytic reduction of carbon dioxide over ZnFe2O4/TiO2 nanobelts heterostructure in cyclohexanol, J. Colloid Interface Sci. 442 (2015) 60–66.
[25] G. Rekhila, M. Trari, Y. Bessekhouad, Characterization and application of the hetero-junction ZnFe2O4/TiO2 for Cr(VI) reduction under visible light, Appl. Water Sci. 7 (2017) 1273–1281.
[26] Z.K. Ghouri, S. Al-Meer, N.A. Barakat, H.Y. Kim, ZnO@ C (core@ shell) microspheres derived from spent coffee grounds as applicable non-precious electrode material for DMFCs, Sci. Rep. 7 (2017).
[27] C.-S. Chou, F.-C. Chou, J.-Y. Kang, Preparation of ZnO-coated TiO 2 electrodes using dip coating and their applications in dye-sensitized solar cells, Powder Technol. 215 (2012) 38–45.
[28] T.-Y. Cho, K.-W. Ko, S.-G. Yoon, S.S. Sekhon, M.G. Kang, Y.-S. Hong, C.-H. Han, Efficiency enhancement of flexible dye-sensitized solar cell with sol–gel formed Nb 2 O 5 blocking layer, Curr. Appl. Phys. 13 (2013) 1391–1396.
[29] G. Kumara, K. Tennakone, V. Perera, A. Konno, S. Kaneko, M. Okuya, Suppression of recombinations in a dye-sensitized photoelectrochemical cell made from a film of tin IV oxide crystallites coated with a thin layer of aluminium oxide, J. Phys. D Appl. Phys. 34 (2001) 868.
[30] T.-V. Nguyen, H.-C. Lee, M.A. Khan, O.-B. Yang, Electrodeposition of TiO 2/SiO 2 nanocomposite for dye-sensitized solar cell, Sol. Energy 81 (2007) 529–534.
[31] P.S. Saud, B. Pant, A.P. Twari, Z.K. Ghouri, M. Park, H.-Y. Kim, Effective photocatalytic efficacy of hydrothermally synthesized silver phosphate decorated titanium dioxide nanocomposite fibers, J. Colloid Interface Sci. 465 (2016) 225–232.
[32] M.A. Khan, M. Shaheer Akhtar, O.B. Yang, Synthesis, characterization and application of sol–gel derived mesoporous TiO2 nanoparticles for dye-sensitized solar cells, Sol. Energy 84 (2010) 2195–2201.
[33] J. Shen, B. Yan, M. Shi, H. Ma, N. Li, M. Ye, One step hydrothermal synthesis of TiO 2-reduced graphene oxide sheets, J. Mater. Chem. 21 (2011) 3415–3421.
[34] K. Vijayalakshmi, D. Sivaraj, Synergistic antibacterial activity of barium doped TiO 2 nanoclusters synthesized by microwave processing, RSC Adv. 6 (2016) 9663–9671.

[35] Y. Zhang, Q. Shi, J. Schliesser, B.F. Woodfield, Z. Nan, Magnetic and thermodynamic properties of nanosized Zn ferrite with normal spinal structure synthesized using a facile method, Inorg. Chem. 53 (2014) 10463–10470.
[36] M. Florea, M. Alifanti, V.I. Parvulescu, D. Mihaila-Tarabasanu, L. Diamandescu, M. Feder, C. Negrila, L. Frunza, Total oxidation of toluene on ferrite-type catalysts, Catal. Today 141 (2009) 361–366.
[37] W. Nuansing, S. Ninmuang, W. Jarernboon, S. Maensiri, S. Seraphin, Structural characterization and morphology of electrospun TiO 2 nanofibers, Mater. Sci. Eng. B 131 (2006) 147–155.
[38] A. Orendorz, A. Brodyanski, J. Lösch, L. Bai, Z. Chen, Y. Le, C. Ziegler, H. Gnaser, Phase transformation and particle growth in nanocrystalline anatase TiO 2 films analyzed by X-ray diffraction and Raman spectroscopy, Surf. Sci. 601 (2007) 4390–4394.
[39] C. Tekmen, A. Suslu, U. Cocen, Titania nanofibers prepared by electrospinning, Mater. Lett. 62 (2008) 4470–4472.
[40] U. Mehmood, Z. Malaibari, F.A. Rabani, A.U. Rehman, S.H.A. Ahmad, M.A. Atieh, M.S. Kamal, Photovoltaic improvement and charge recombination reduction by aluminum oxide impregnated MWCNTs/TiO 2 based photoanode for dye-sensitized solar cells, Electrochim. Acta 203 (2016) 162–170.
[41] S. Xu, D. Feng, W. Shangguan, Preparations and photocatalytic properties of visible-light-active zinc ferrite-doped TiO2 photocatalyst, J. Phys. Chem. C 113 (2009) 2463–2467.
[42] Y. Hou, X. Li, Q. Zhao, X. Quan, G. Chen, Electrochemically assisted photocatalytic degradation of 4-chlorophenol by ZnFe2O4−Modified TiO2 nanotube array electrode under visible light irradiation, Environ. Sci. Technol. 44 (2010) 5098–5103.